

Original Article

OH-Radical Oxidation of Lung Surfactant Protein B on Aqueous Surfaces

Shinichi Enami^{*1} and Agustín J. Colussi²

¹National Institute for Environmental Studies, 16-2 Onogawa, Tsukuba, Ibaraki 305-8506, Japan

²Linde Center for Global Environmental Science, California Institute of Technology, California 91125, U.S.A.

Air pollutants generate reactive oxygen species on lung surfaces. Here we report how hydroxyl radicals ($\cdot\text{OH}$) injected on the surface of water react with SP-B₁₋₂₅, a 25-residue polypeptide surrogate of human lung surfactant protein B. Our experiments consist of intersecting microjets of aqueous SP-B₁₋₂₅ solutions with O₃/O₂/H₂O/N₂(g) gas streams that are photolyzed into $\cdot\text{OH}(\text{g})$ *in situ* by 266 nm laser nanosecond pulses. Surface-sensitive mass spectrometry enables us to monitor the prompt (<10 μs) and simultaneous formation of primary O_n-containing products/intermediates ($n \leq 5$) triggered by the reaction of $\cdot\text{OH}$ with interfacial SP-B₁₋₂₅. We found that O-atoms from both O₃ and $\cdot\text{OH}$ are incorporated into the reactive cysteine Cys₈ and Cys₁₁ and tryptophan Trp₉, components of the hydrophobic N-terminus of SP-B₁₋₂₅ that lies at the topmost layers of the air-liquid interface. Remarkably, these processes are initiated by $\cdot\text{OH}$ additions rather than by H-atom abstractions from S-H, C-H, or N-H groups. By increasing the hydrophilicity of the N-terminus region of SP-B₁₋₂₅, these transformations will impair its role as a surfactant.



Copyright © 2018 Shinichi Enami and Agustín J. Colussi. This is an open access article distributed under the terms of Creative Commons Attribution License, which permits use, distribution, and reproduction in any medium, provided the original work is properly cited and is not used for commercial purposes.

Please cite this article as: Mass Spectrom (Tokyo) 2018; 7(2): S0077

Keywords: air pollution, lung surfactant, reactive oxygen species, interfacial reaction, protein

(Received August 21, 2018; Accepted October 11, 2018)

INTRODUCTION

Human lung alveoli are covered by a 0.1–0.5 μm thick epithelium lining fluid (ELF) that has a large surface area ~885,000 cm² (vs. the ~4,500 cm² of the airway).¹ ELF contains surfactant proteins B and C (~10 wt% of total ELF surfactant material),¹⁻⁶ in addition to water-soluble antioxidants such as glutathione ([GSH] ~100–500 μM), ascorbic acid ([Asc] ~100 μM),^{1,7} uric acid, and liposoluble α -tocopherol.⁷⁻¹¹ SP-B functions reduce the energy required to expand lungs during aspiration and prevent their collapse upon exhalation.¹² A recent simulation study revealed that SP-B induces the formation of bilayer reservoirs by monolayer folding, helps attaching the disconnected bilayer aggregates to a monolayer at the air-water interface, and facilitates lipid transfer between these structures.¹³ SP-B deficiency is known to cause severe lung dysfunction and inflammation.¹⁴ Human infants genetically lacking SP-B cannot survive.¹⁵ It is apparent that the oxidative degradation of SP-B's surface activity should induce acute syndromes.^{2,16-19}

Recent studies suggested that the inhalation of particulate matter (PM) produces $\cdot\text{OH}$ in ELF.²⁰⁻²² *In vivo* studies have shown that $\cdot\text{OH}$ produced in ELF exposed to O₃(g) enhances bronchoalveolar permeability.²³ Given the abundance of antioxidants in ELF (see above), SP-B oxidative

damage can be triggered only by $\cdot\text{OH}$ produced or deposited close to SP-B.²⁴ Because inhaled gas-phase oxidants are very reactive and the SP-B surfactant is present at the ELF surface, *the relevant reactive events are expected to take place at the air-water interface rather than in the bulk liquid.* A previous study found that the heterogeneous reaction of O₃(g) with SP-B₁₋₂₅ (a model 25-residue polypeptide of human SP-B)²⁵ in water-methanol droplets yields several products that incorporate O-atoms in a few seconds.³ The products from the droplets exposed to O₃(g) or the solution treated O₃-bubbling were found to be quite different,³ implying that the mechanism at the gas-liquid interface is different from that in bulk solution.⁷ The authors also generated reactive intermediates in bulk water with Fenton's reagent (Fe²⁺+H₂O₂) to test whether the chemistry actually involved $\cdot\text{OH}$ radicals. However, we recently found that the Fenton reaction at the air-water interface produces oxo-ferryl species (Fe^{IV}=O) in high yields, which behave as O-atom donors rather than as H-abstrating species.²⁶⁻³⁰ In fact, a recent study suggested that Fenton's reaction produces <10% $\cdot\text{OH}$ in bulk water at physiological pH 6-7.²⁸ Since the production of Fe^{IV}=O is significantly enhanced in Fenton's reaction at the air-water interface,²⁶ establishing the mechanism of the oxidation of SP-B₁₋₂₅ initiated by $\cdot\text{OH}$ at the air-water interface requires experiments involving a

*Correspondence to: Shinichi Enami, National Institute for Environmental Studies, 16-2 Onogawa, Tsukuba, Ibaraki 305-8506, Japan, e-mail: enami.shinichi@nies.go.jp

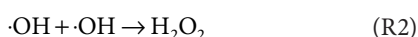
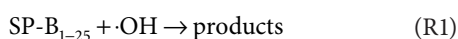
direct, *bona fide* source of $\cdot\text{OH}$ *in situ*.

In this paper we report a mass-spectrometric study specifically designed to address these issues, in which aqueous SP-B₁₋₂₅ (a 25-residue polypeptide NH₂-¹FPIPLPYCWLCRALIKRIQAMIPK²⁵G-COOH) reacts with gas-phase $\cdot\text{OH}$ at the air–water interface. SP-B₁₋₂₅ has been used as a representative model peptide that mimics SP-B functions, because of the similarity of their chemical and physical properties.^{4,6} Our experiments were conducted in a novel setup in which aqueous SP-B₁₋₂₅ microjets were intersected with gas-phase $\cdot\text{OH}$ streams generated in close proximity to the surface *via* pulsed laser photolysis of O₃(g)/H₂O(g)/O₂(g)/N₂(g) mixtures,³¹⁻³⁶ while continuously monitoring the composition of the interfacial layers of the microjets *via* pneumatic ionization mass spectrometry.³⁷⁻³⁹

EXPERIMENTAL SECTION

The present experimental setup is essentially the same as the one reported elsewhere.³¹ The charged product species generated on the surface of SP-B₁₋₂₅(aq) microjets during $\tau \sim 10 \mu\text{s}$ contact times (τ is the lifetime of the microjets before being pneumatically nebulized) with O₃(g) or $\cdot\text{OH}$ (g) streams are monitored *in-situ* by online mass spectrometry (Fig. S1, Agilent 6130 Quadrupole LC/MS Electrospray System).³¹ O(¹D) generated by 266 nm photons reacts with excess H₂O(g) ([H₂O(g)] $\sim 7.6 \times 10^{17}$ molecule cm⁻³) to form $\cdot\text{OH}$ radicals within ~ 6 ns (from $k_1(\text{O}^1\text{D})+\text{H}_2\text{O})=2.2 \times 10^{-10}$ cm³ molecule⁻¹ s⁻¹) (see [$\cdot\text{OH}$ (g)] estimates in SI). These conditions ensure that the detected species correspond to the truly initial stages of reaction.³⁴⁻³⁶ The all-¹²C isotopomer of SP-B₁₋₂₅ ≡ Phe₁-Pro₂-Ile₃-Pro₄-Leu₅-Pro₆-Tyr₇-Cys₈-Trp₉-Leu₁₀-Cys₁₁-Arg₁₂-Ala₁₃-Leu₁₄-Ile₁₅-Lys₁₆-Arg₁₇-Ile₁₈-Gln₁₉-Ala₂₀-Met₂₁-Ile₂₂-Pro₂₃-Lys₂₄-Gly₂₅, has a molecular mass of 2928 Da. Samples are injected at 100 $\mu\text{L min}^{-1}$ into the spraying chamber of the mass spectrometer through a grounded stainless steel needle (100 μm bore) coaxial with a sheath issuing nebulizer N₂(g) at a high velocity ($v_g \approx 160$ m/s).³⁸ The surface specificity of our experiments has been demonstrated previously.^{26,37,38,40,41} It should be emphasized that the products we observe are formed when gaseous reactants collide with the intact aqueous jets as they emerge from the nozzle, *i.e.*, before jets are broken up into sub-micron charged droplets by the nebulizer gas.²⁶ Since 266 nm pulses flash every 100 ms, and the microjets breaks up within $\sim 10 \mu\text{s}$ after being ejected from the nozzle, it is safe to assume that the observed phenomena always take place on the surface of fresh solutions.³¹

We verified that in the absence of O₃(g) neither reactant signals are affected nor new product signals appear upon 266 nm pulsed irradiation, thereby excluding the photolysis SP-B₁₋₂₅ (aq) as the source of detected products (see Fig. S2). In our experiments, $\cdot\text{OH}$ (g) will stick to the surface of water in nearly every collision,^{31,33-35,42-46} and react with SP-B₁₋₂₅ (R1), or dimerize into H₂O₂ (R2) at the air–water interface.



The preference of $\cdot\text{OH}$ for interfacial layers relative to the bulk liquid is supported both by theoretical and experimen-

tal studies.^{31,32,34,43-46} This effect should enhance the probability of $\cdot\text{OH}$ reactions with hydrophobic residues at the air–water interface before it diffuses into bulk phase.

RESULTS AND DISCUSSION

Figure 1A shows a positive ion mass spectrum of 43 μM SP-B₁₋₂₅(aq) microjets exposed to O₂(g)/H₂O(g)/N₂(g), and to O₃(g)/O₂(g)/H₂O(g)/N₂(g) with the 266 nm laser on and off. The three major peaks at $m/z=586.7$, 733.0 and 977.0 correspond to multiply protonated [SP-B₁₋₂₅+ m H] ^{$m+$} for $m=5$, 4 and 3, respectively. It is apparent that [SP-B₁₋₂₅+4 H]⁴⁺ [NH₂-FPIPLPYCWLCR(H⁺)ALIK(H⁺)-R(H⁺)IQAMIPK(H⁺)G-COOH]⁴⁺ is the most abundant species under present conditions. We found that the relative abundances of the most protonated species increase at lower SP-B₁₋₂₅(aq) concentrations (Fig. S3), a phenomenon that we tentatively ascribe to decreased repulsion among sparser polycationic chains in the air–water interfacial layers sampled by our technique. Hereafter, our analysis will largely focus on the evolution of the $m/z^+=733.0$ [SP-B₁₋₂₅+4 H]⁴⁺ species upon variations of experimental conditions.

All [SP-B₁₋₂₅+ m H] ^{$m+$} signals decrease and new products appear (Figs. 1A and 1B, blue trace) in the presence of O₃(g) without 266 nm. Thus, SP-B₁₋₂₅ is found to be reactive toward O₃, in accordance with literature reports.^{3,6,47}

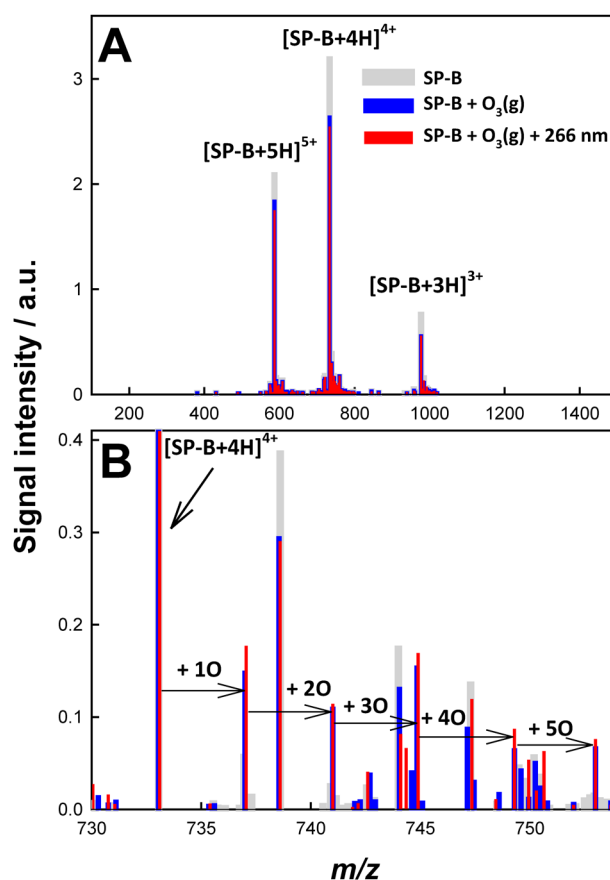


Fig. 1. A) Positive ion mass spectra of aqueous 43 μM SP-B₁₋₂₅ microjets in O₂(g)/H₂O(g)/N₂(g) mixtures (gray), or exposed to ~ 500 ppmv O₃(g) in O₂(g)/H₂O(g)/N₂(g) mixtures in the absence (blue)/in the presence (red) of 40 mJ 266 nm pulses. 1 ppmv = 2.46×10^{13} molecules cm⁻³. B) Spectra of [SP-B₁₋₂₅+4 H]⁴⁺ and its oxidation products in the 730–760 Da range.

In Fig. 1B, the $m/z^+=737=[2928+4(+4\text{ H})+16(+\text{O})]/4$ signal is assigned to $[\text{SP-B}_{1-25}+4\text{H}+\text{O}]^{4+}$. The $m/z^+=741=[2928+4(+4\text{ H})+32(+2\text{O})]/4$ signal is $[\text{SP-B}_{1-25}+4\text{ H}+2\text{ O}]^{4+}$, i.e., $m/z^+=733+4n$ is $[\text{SP-B}_{1-25}+4\text{ H}+n\text{ O}]^{4+}$ ($n=1-5$). We did not detect $n\geq 6$ products in our experiments. Importantly, the application of 266 nm laser pulses *enhances* all product signals (Fig. 1B, red trace), thereby suggesting that the detectable products of SP-B_{1-25} oxidation by O_3 and $\cdot\text{OH}$ might be identical. This finding is in accordance with previous reports on the ozonation of amino acids,⁴⁸⁾ and the $\cdot\text{OH}$ -initiated oxidation of proteins.⁴⁹⁾

Figure 2 shows $[\text{SP-B}_{1-25}+4\text{ H}+n\text{ O}]^{4+}$ mass spectral signal intensities from $\text{SP-B}_{1-25}(\text{aq})$ microjets exposed to $\text{O}_3(\text{g})/\text{O}_2(\text{g})/\text{H}_2\text{O}(\text{g})/\text{N}_2(\text{g})$ mixtures under on and off 266 nm pulses as functions of $[\text{O}_3(\text{g})]$. It is apparent that

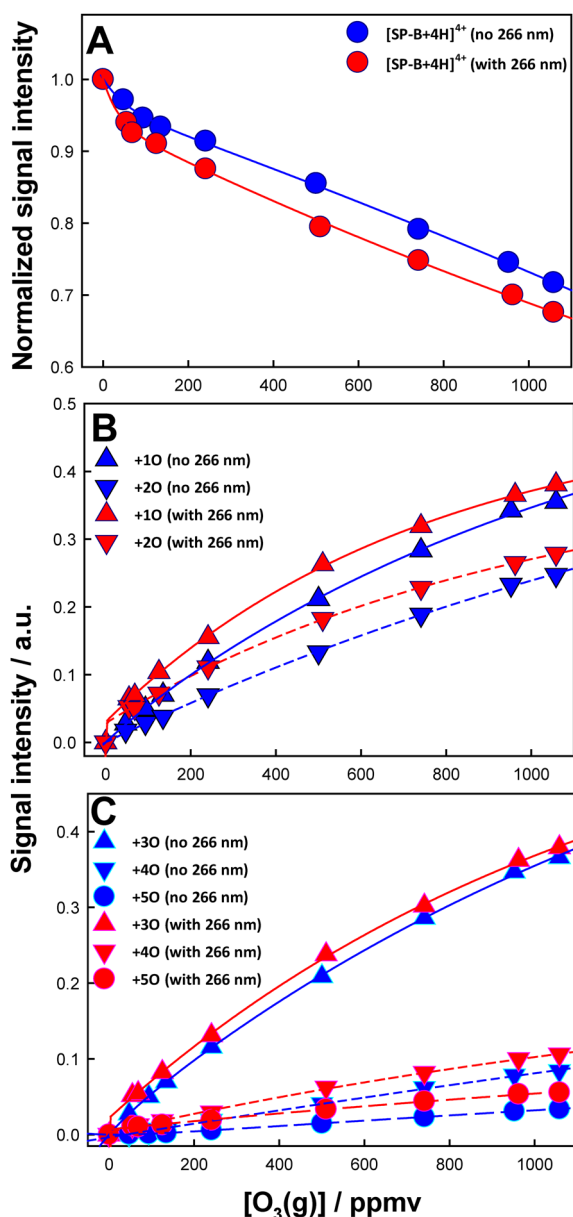


Fig. 2. Reactant (A) and products (B, C) mass spectral signal intensities from aqueous $43\ \mu\text{M}$ SP-B_{1-25} microjets exposed to $\text{O}_3(\text{g})/\text{O}_2(\text{g})/\text{H}_2\text{O}(\text{g})/\text{N}_2(\text{g})$ mixtures in the absence (blue) or presence (red) of 266 nm laser beams (40 mJ pulse^{-1}) as a function of the $\text{O}_3(\text{g})$ mixing ratio; $1\text{ ppmv}=2.46\times 10^{13}$ molecules cm^{-3} .

the depletion of SP-B_{1-25} is more extensive and $[\text{SP-B}_{1-25}+4\text{ H}+n\text{ O}]^{4+}$ ($n=1-5$) production is enhanced upon irradiation. Note the simultaneous appearance of all $n=1-5$ $[\text{SP-B}_{1-25}+4\text{ H}+n\text{ O}]^{4+}$ products (see below). Figure S4 compares the bi-exponential depletion of $[\text{SP-B}_{1-25}+3\text{ H}]^{3+}$, $[\text{SP-B}_{1-25}+4\text{ H}]^{4+}$ and $[\text{SP-B}_{1-25}+5\text{ H}]^{5+}$ signal intensities under the same conditions of Fig. 2. The fact that the extent of $[\text{SP-B}_{1-25}+3\text{ H}]^{3+}$ depletion is significantly larger than for the other protonated species suggests structural changes that depend on m .⁵⁰⁻⁵²⁾ Species of smaller m values behave as if they increase the exposure of the more hydrophobic (surface-active) amino acid residues to O_3 and $\cdot\text{OH}$. This is consistent with experiments showing that more hydrophobic long-chain species react more extensively with $\cdot\text{OH}(\text{g})$ than the less hydrophobic shorter-chain ones.^{31,32,34,35)} This is also consistent with a recent report showing that antioxidant activity of free amino acids in Fenton's reaction increases with

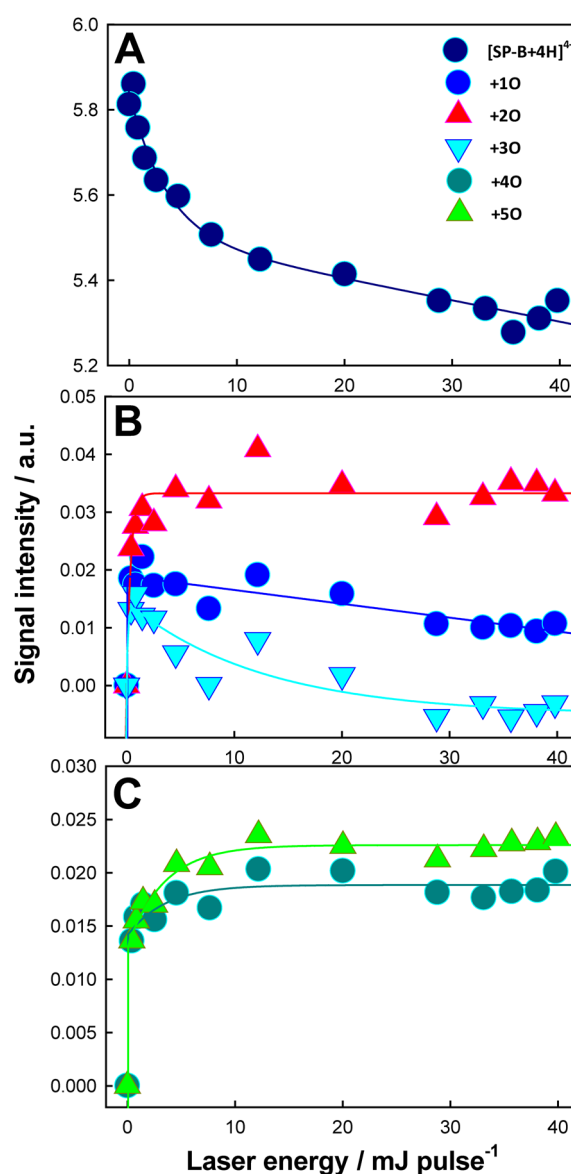


Fig. 3. Reactant (A) and products (B, C) mass spectral signal intensities from aqueous $43\ \mu\text{M}$ SP-B_{1-25} microjets exposed to $\text{O}_3(\text{g})/\text{O}_2(\text{g})/\text{H}_2\text{O}(\text{g})/\text{N}_2(\text{g})$ mixtures at $[\text{O}_3(\text{g})] \sim 600\text{ ppmv}$, irradiated with 266 nm laser beams as functions of laser energy (in mJ pulse^{-1}). Background (before pulsing at 266 nm) products signals were subtracted.

hydrophobicity.⁵³⁾

Figure 3 shows reactant decay and product enhancements upon irradiation in similar experiments as functions of 266 nm pulse energy. In Fig. 3, laser energies (x -axis) at 1, 5, 10, 20, 30, and 40 mJ pulse⁻¹ correspond to $[\cdot\text{OH}(\text{g})]_0 \approx 2, 9, 18, 33, 46,$ and 57 ppmv, respectively. The actual $[\cdot\text{OH}]$ colliding to the microjets are expected to be smaller than these estimated values.^{34,35)} It is apparent that the full extent of irradiation effects is already reached at the lowest pulse energies. Further increases in pulse energy only achieve the partial degradation of the $n=1$ and 3 $[\text{SP-B}_{1-25} + 4 \text{ H} + n \text{ O}]^{4+}$ products. $[\text{SP-B}_{1-25} + 4 \text{ H} + 3 \text{ O}]^{4+}$ in particular disappears above ~ 20 mJ pulse, possibly *via* photo-degradation or secondary reactions. The effect of laser energy on product formation (Fig. 3) is markedly different from that observed upon variations of $[\text{O}_3(\text{g})]$ (Fig. 2): SP-B_{1-25} decays bi-exponentially as a function of laser energy, while some products reach steady state at the lowest fluences, such as $[\text{SP-B}_{1-25} + 4 \text{ H} + 2 \text{ O}]^{4+}$, or are degraded, such as $[\text{SP-B}_{1-25} + 4 \text{ H} + \text{O}]^{4+}$ and $[\text{SP-B}_{1-25} + 4 \text{ H} + 3 \text{ O}]^{4+}$, at larger fluences.

Our results are consistent with the rapid incorporation of up to 5 O-atoms to SP-B_{1-25} by both O_3 and $\cdot\text{OH}$ at the air–water interface. Since (i) the reported rate constants for the reactions of cysteine ($k_{\text{Cys}+\text{ozone}} > 7.0 \times 10^6 \text{ M}^{-1} \text{ s}^{-1}$) and tryptophan ($k_{\text{Trp}+\text{ozone}} = 7.0 \times 10^6 \text{ M}^{-1} \text{ s}^{-1}$) with O_3 in bulk water are $> 10^2$ times larger than for the rest of the amino acids (except for methionine),⁴⁸⁾ (ii) the corresponding reactions with $\cdot\text{OH}$ ($k_{\text{Trp}+\cdot\text{OH}} = 1.3 \times 10^{10} \text{ M}^{-1} \text{ s}^{-1}$), ($k_{\text{Cys}+\cdot\text{OH}} = 3.5 \times 10^{10} \text{ M}^{-1} \text{ s}^{-1}$) are diffusionally controlled, (iii) both cysteines Cys_8 and Cys_{11} , and tryptophan Trp_9 , are embedded in the hydrophobic section of SP-B_{1-25} that resides at the topmost layers of air–water interface,^{3,54)} we infer that these are the three amino acid residues attacked by both O_3 and $\cdot\text{OH}$. More specifically, we envision that in the initial stages of the oxidation process O_3 will transfer one O-atom to the sulfhydryl R-S-H group of Cys to produce the corresponding sulfenic acid R-S-OH,⁵⁵⁾ whereas O_3 also adds to the pyrrole ring of Trp to produce the corresponding primary POZ and secondary SOZ Trp-O_3 ozonides (Scheme S1). We also consider that the S-containing methionine Met_{21} residue,⁵⁶⁾ by being situated in the hydrophilic C-terminal side buried in water (as shown by MD simulations by Goddard and coworkers),³⁾ is less likely to be oxidized by both O_3 and $\cdot\text{OH}$ than the Cys residues closer to the air–water interface. The fact that both O_3 and $\cdot\text{OH}$ preferably reside at the air–water interface rather than in bulk^{44–46)} makes it less likely that they will diffuse towards the Met_{21} residue located in bulk.

We also tested whether the mechanism of Trp ozonation at the air–water interface follows the same course as in bulk water in our experimental setup by exposing free L-tryptophan (aq) to $\text{O}_3(\text{g})/\text{O}_2(\text{g})/\text{H}_2\text{O}(\text{g})/\text{N}_2(\text{g})$ mixtures in the absence/presence of 266 nm pulses (Fig. S5). We found that the interfacial ozonation of anionic L-tryptophan ($m/z^- = 203$) produces species that incorporate one to three O-atoms, which are detected at $m/z^- = 219$ (+1O), 235 (+2O) and 251 (+3O), along with a signal at $m/z^- = 207$. These species match the masses of the reported products of Trp ozonation^{3,57)} and hydroxylation^{58,59)} in bulk water. See Scheme S1 for assignments. We note, however, that the formation of kynurenine (Kyn) from the oxidation of Trp_9 in SP-B_{1-25} , which would have led to a

peak at $m/z^+ = 734 = [2928 + 48 (+3\text{O}) - 44 (-\text{CO}_2) + 4 (+4\text{H})]/4$, is absent from our mass spectra (Fig. 1B). Thus, from the fact that we observe the incorporation of up to 5 O-atoms into SP-B_{1-25} , we conclude that Trp_9 accepts 3 O-atoms, and Cys_8 and Cys_{11} one O-atom each during the ozonation and hydroxylation of SP-B_{1-25} at the air–water interface under present conditions. Note that H-abstraction from Trp by $\cdot\text{OH}$ in the presence of O_2 would have led to the formation of a peroxy radical, $m/z^- = 203 - 1 (-\text{H}) + 32 (+\text{O}_2) = 234$, and possibly to an alcohol $m/z^- = 234 - 16 + 1 = 219$, and carbonyl $m/z^- = 234 - 16 - 1 = 217$, from the disproportionation of the peroxy radical, as in the case of alkyl and aromatic carboxylic acids.^{31,32,34,35)} Their conspicuous absence proves that under present conditions all oxidation processes, both those initiated by ozonation and hydroxylation, are initiated by O-atom transfers or $\cdot\text{OH}$ additions to the S-center of the Cys and the pyrrole ring of Trp, rather than by H-atom abstraction from the myriad C–H bonds available in SP-B_{1-25} . The exceptional reactivity of S-atoms in biomolecules for $\cdot\text{OH}$ -addition is consistent with our $\text{GSH} + \cdot\text{OH}$ and $\text{GSSG} + \cdot\text{OH}$ studies at the air–water interface,³⁶⁾ suggesting that interface-specific phenomena are general and stem from the peculiar nature of interfacial water as a reaction medium.^{26,60–62)} We also note that these highly selective oxidations imply “molecular recognition” processes, possibly mediated by water networks.^{63,64)} Thus, our results suggest that these hitherto unknown interface-specific radical recognition processes may play central roles in lung surface chemistry.

The occurrence of up to 5 O-atom transfers to a single SP-B_{1-25} unit implies that oxidants are always in excess over reactive centers at the interface. Thus, the initial attack on any one of them is followed by additional, successive O-atom transfers until all such centers reach their limiting degree of oxidation during contact times. However, since we have shown that GSH and free cysteine can add up to 3 O-atoms under similar conditions,^{36,55)} it appears that first-generation sulfenic acids $\text{S}(\text{O})\text{-H}$ are not further oxidized in SP-B_{1-25} . This is because they may rapidly form S–S bridges or, due to conformational changes, they become buried in the hydrophilic segment of the polypeptide.⁶⁵⁾ In this context, we note that the fate of sulfenic acid could be determined by the microenvironment.^{65,66)} For example, a S–OH can persist for several hours in human serum albumin, in which 34 of 35 cysteine-residues can create disulfide-bonds thereby minimizing the number of available reduced S-atoms.⁶⁷⁾ Another study revealed that the hypervalent S-atoms of sulfenic acids can form covalent complexes with the N-atoms of neighboring histidine residues, a phenomenon that prevents the over-oxidation of cysteine sulfenic acid.⁶⁸⁾ Therefore, it is conceivable that neighboring Trp_9 's indole-N-atoms may stabilize the $\text{Cys}_8\text{-OH}$ and $\text{Cys}_{11}\text{-OH}$ in a similar way. An additional effect is that since sulfenic $\text{S}(\text{O})_2\text{-H}$ ($\text{p}K_a \approx 2$) and sulfonic acids $\text{S}(\text{O})_2\text{-OH}$ ($\text{p}K_a < 1$) are much more acidic than $\text{S}(\text{O})\text{-H}$ ($\text{p}K_a \approx 7.6$),⁵⁵⁾ they would deprotonate at $\text{pH} \sim 6$ thereby decreasing the net charge of $[\text{SP-B}_{1-25} + m \text{ H} + \text{O}]^{m+}$ from $m \rightarrow (m-1)$ and shifting the mass signals. However, the fact that we did not observe such behavior (Fig. S3) led us to exclude the oxidation of Cys-sulfenic acid residues.

The mechanism of SP-B_{1-25} oxidations shown here is generally consistent with previous studies.^{3,6,47)} However,

the previous report using the Fenton reaction for oxidizing SP-B₁₋₂₅ by ·OH in bulk water showed O_n-products up to n=10, which is in contrast with our observations (n=1–5).³⁾ We ascribe this to the following reasons: 1) differences between bulk vs. interfacial mechanism, 2) the very different time scales between the two systems, and 3) the Fenton reaction may largely produce oxo-ferryls rather than ·OH. First, as observed in GSH/GSSH+·OH experiments,³⁶⁾ the difference indeed comes from where the ·OH-reaction occurs, that is, in water vs. at the air–water interface. We recently reported that ·OH-reaction of amphiphilic species are remarkably different in bulk water vs. at the air–water interface.^{32,34,35)} Second, in the previous report the measurement was performed >12h after the Fenton reaction starts,³⁾ while in the present study the time scale is <10 μs. Third, as mentioned above, the Fenton reaction may produce oxo-ferryl species in >90% yields in bulk water at pH 6–7,²⁸⁾ and even more so at the air–water interface.²⁶⁾ In the present work, ·OH is generated by well-established gas-phase photo-reactions.³¹⁾

Hydroxylation, by increasing the hydrophilicity of the N-terminus, is generally expected to degrade the tensioactive properties of SP-B.^{6,47,69)} The formation of intra/intermolecular S–S bonding *via* sulfenic R–S–OH groups, that likely occurs in a longer time scale, could also disturb SP-B function as surfactant.^{5,6,13)} Since inhalation of PM and O₃ evidently induces reactive oxygen species (ROS) in ELF of our lungs,²⁰⁾ the present results are directly linked to adverse health effects of air pollutants impairing the role of SP-B as the surfactant.

CONCLUSION

We report a mass spectrometric study on how aqueous SP-B₁₋₂₅ is oxidized by O₃ and ·OH at the air–water interface. By using a novel method that combines online pneumatic ionization mass spectrometry with pulse laser flash photolysis,³¹⁾ we were able to detect the intermediates/products generated in the initial stages of the oxidation of SP-B₁₋₂₅ by ·OH on water surfaces. Our results suggest that two Cys-residues and a Trp-residue in hydrophobic N-terminal side are the major targets for both O₃ and ·OH, rather than H-atom abstraction from the multiple C–H/N–H bonds available in SP-B₁₋₂₅. We infer that this remarkable interface-specific radical recognition process is what determines the observed chemistry. These chemical transformations increase the polarity of the SP-B₁₋₂₅ hydrophobic section, promote the formation of disulfide links therein and, therefore, are deemed to impair its role as the surfactant that prevents lung collapse upon expiration.

SUPPORTING INFORMATION AVAILABLE

Additional data and experimental details. This material is available free of charge *via* the Internet.

Acknowledgements

S. E. is grateful to the Japan Science and Technology Agency (JST) PRESTO program and the Research Foundation for Opto-Science and Technology. S. E. is indebted to Prof. Hiroshi Masuhara for his kind advices.

A. J. C. acknowledges support from the National Science Foundation USA, grant AGS-1744353.

REFERENCES

- 1) C. E. Cross, A. van der Vliet, S. Louie, J. J. Thiele, B. Halliwell. Oxidative stress and antioxidants at biosurfaces: Plants, skin, and respiratory tract surfactants. *Environ. Health Perspect.* 106(Suppl. 5): 1241–1251, 1998.
- 2) B. Müller, C. Seifart, P. J. Barth. Effect of air pollutants on the pulmonary surfactant system. *Eur. J. Clin. Invest.* 28: 762–777, 1998.
- 3) H. I. Kim, H. Kim, Y. S. Shin, L. W. Beegle, S. S. Jang, E. L. Neidholdt, W. A. Goddard, J. R. Heath, I. Kanik, J. L. Beauchamp. Interfacial reactions of ozone with surfactant protein B in a model lung surfactant system. *J. Am. Chem. Soc.* 132: 2254–2263, 2010. doi: 10.1021/ja908477w
- 4) M. L. Longo, A. M. Bisagno, J. A. N. Zasadzinski, R. Bruni, A. J. Waring. A function of lung surfactant protein SP-B. *Science* 261: 453–456, 1993. doi: 10.1126/science.8332910
- 5) J. Pérez-Gil. Structure of pulmonary surfactant membranes and films: The role of proteins and lipid–protein interactions. *Biochim. Biophys. Acta* 1778: 1676–1695, 2008. doi: https://doi.org/10.1016/j.bbame.2008.05.003
- 6) J. M. Hemming, B. R. Hughes, A. R. Rennie, S. Tomas, R. A. Campbell, A. V. Hughes, T. Arnold, S. W. Botchway, K. C. Thompson. Environmental pollutant ozone causes damage to lung surfactant protein B (SP-B). *Biochemistry* 54: 5185–5197, 2015. doi: 10.1021/acs.biochem.5b00308
- 7) S. Enami, M. R. Hoffmann, A. J. Colussi. Acidity enhances the formation of a persistent ozonide at aqueous ascorbate/ozone gas interfaces. *Proc. Natl. Acad. Sci. U.S.A.* 105: 7365–7369, 2008. doi: 10.1073/pnas.0710791105
- 8) S. Enami, A. R. Hoffmann, A. J. Colussi. Ozonolysis of uric acid at the air/water interface. *J. Phys. Chem. B* 112: 4153–4156, 2008.
- 9) S. Enami, M. R. Hoffmann, A. J. Colussi. How phenol and alpha-tocopherol react with ambient ozone at gas/liquid interfaces. *J. Phys. Chem. A* 113: 7002–7010, 2009. doi: 10.1021/jp901712k
- 10) S. Enami, M. R. Hoffmann, A. J. Colussi. Absorption of Inhaled NO₂. *J. Phys. Chem. B* 113: 7977–7981, 2009. doi: 10.1021/jp902667x
- 11) H. I. Kim, H. Kim, Y. S. Shin, L. W. Beegle, W. A. Goddard, J. R. Heath, I. Kanik, J. L. Beauchamp. Time resolved studies of interfacial reactions of ozone with pulmonary phospholipid surfactants using field induced droplet ionization mass spectrometry. *J. Phys. Chem. B* 114: 9496–9503, 2010. doi: 10.1021/jp102332g
- 12) S. Hawgood, K. Shiffer. Structures and properties of the surfactant-associated proteins. *Annu. Rev. Physiol.* 53: 375–394, 1991. doi: 10.1146/annurev.ph.53.030191.002111
- 13) S. Baoukina, D. P. Tieleman. Lung surfactant protein SP-B promotes formation of bilayer reservoirs from monolayer and lipid transfer between the interface and subphase. *Biophys. J.* 100: 1678–1687, 2011. doi: 10.1016/j.bpj.2011.02.019
- 14) M. Ikegami, J. A. Whitsett, P. C. Martis, T. E. Weaver. Reversibility of lung inflammation caused by SP-B deficiency. *Am. J. Physiol. Lung Cell. Mol. Physiol.* 289: L962–L970, 2005. doi: 10.1152/ajplung.00214.2005
- 15) L. M. Noguee, G. Garnier, H. C. Dietz, L. Singer, A. M. Murphy, D. E. deMello, H. R. Colten. A mutation in the surfactant protein B gene responsible for fatal neonatal respiratory disease in multiple kindreds. *J. Clin. Invest.* 93: 1860–1863, 1994. doi: 10.1172/JCI117173
- 16) R. Banerjee. Surface chemistry of the lung surfactant system: Techniques for *in vitro* evaluation. *Curr. Sci.* 82: 420–428, 2002.
- 17) J. G. Fernsler, J. A. Zasadzinski. Competitive adsorption: A physical model for lung surfactant inactivation. *Langmuir* 25: 8131–8143, 2009. doi: 10.1021/la8039434

- 18) F. J. Kelly, S. Birch. Pulmonary protein-synthesis response to ozone. *Hum. Exp. Toxicol.* 13: 407–410, 1994.
- 19) M. C. Williams, S. Hawgood, R. L. Hamilton. Changes in lipid structure produced by surfactant proteins SP-A, SP-B, and SP-C. *Am. J. Respir. Cell Mol. Biol.* 5: 41–50, 1991.
- 20) M. Shiraiwa, K. Ueda, A. Pozzer, G. Lammel, C. J. Kampf, A. Fushimi, S. Enami, A. M. Arangio, J. Fröhlich-Nowoisky, Y. Fujitani, A. Furuyama, P. S. J. Lakey, J. Lelieveld, K. Lucas, Y. Morino, U. Pöschl, S. Takahama, A. Takami, H. Tong, B. Weber, A. Yoshino, K. Sato. Aerosol health effects from molecular to global scales. *Environ. Sci. Technol.* 51: 13545–13567, 2017. doi: 10.1021/acs.est.7b04417
- 21) H. Tong, A. M. Arangio, P. S. J. Lakey, T. Berkemeier, F. Liu, C. J. Kampf, W. H. Brune, U. Pöschl, M. Shiraiwa. Hydroxyl radicals from secondary organic aerosol decomposition in water. *Atmos. Chem. Phys.* 16: 1761–1771, 2016. doi: 10.5194/acp-16-1761-2016
- 22) E. Vidrio, C. H. Phuah, A. M. Dillner, C. Anastasio. Generation of hydroxyl radicals from ambient fine particles in a surrogate lung fluid solution. *Environ. Sci. Technol.* 43: 922–927, 2009. doi: 10.1021/es801653u
- 23) D. K. Bhalla. Alteration of ozone-induced airway permeability by oxygen metabolites and antioxidants. *Toxicol. Lett.* 73: 91–101, 1994. doi: 10.1016/0378-4274(94)90099-X
- 24) M. B. Goshe, Y. H. Chen, V. E. Anderson. Identification of the sites of hydroxyl radical reaction with peptides by hydrogen/deuterium exchange: Prevalence of reactions with the side chains. *Biochemistry* 39: 1761–1770, 2000. doi: 10.1021/bi991569j
- 25) M. T. Dohm, S. L. Seuryck-Servoss, J. Seo, R. N. Zuckermann, A. E. Barron. Close mimicry of lung surfactant protein B by “clicked” dimers of helical, cationic peptoids. *Biopolymers* 92: 538–553, 2009. doi: 10.1002/bip.21309
- 26) S. Enami, Y. Sakamoto, A. J. Colussi. Fenton chemistry at aqueous interfaces. *Proc. Natl. Acad. Sci. U.S.A.* 111: 623–628, 2014. doi: 10.1073/pnas.1314885111
- 27) N. Yamamoto, N. Koga, M. Nagaoka. Ferryl-oxo species produced from Fenton’s reagent via a two-step pathway: Minimum free-energy path analysis. *J. Phys. Chem. B* 116: 14178–14182, 2012. doi: 10.1021/jp310008z
- 28) H. Bataineh, O. Pestovsky, A. Bakac. pH-induced mechanistic changeover from hydroxyl radicals to iron(IV) in the Fenton reaction. *Chem. Sci. (Camb.)* 3: 1594–1599, 2012. doi: 10.1039/c2sc20099f
- 29) J. T. Groves. High-valent iron in chemical and biological oxidations. *J. Inorg. Biochem.* 100: 434–447, 2006. doi: 10.1016/j.jinorgbio.2006.01.012
- 30) T. Tsuneda, T. Taketsugu. Theoretical investigations on hydrogen peroxide decomposition in aquo. *Phys. Chem. Chem. Phys.* 20: 24992–24999, 2018. doi: 10.1039/C8CP04299C
- 31) S. Enami, M. R. Hoffmann, A. J. Colussi. *In situ* mass spectrometric detection of interfacial intermediates in the oxidation of RCOOH(aq) by gas-phase OH-radicals. *J. Phys. Chem. A* 118: 4130–4137, 2014.
- 32) S. Enami, M. R. Hoffmann, A. J. Colussi. Stepwise oxidation of aqueous dicarboxylic acids by gas-phase OH radicals. *J. Phys. Chem. Lett.* 6: 527–534, 2015. doi: 10.1021/jz502432j
- 33) S. Enami, Y. Sakamoto, K. Hara, K. Osada, M. R. Hoffmann, A. J. Colussi. “Sizing” heterogeneous chemistry in the conversion of gaseous dimethyl sulfide to atmospheric particles. *Environ. Sci. Technol.* 50: 1834–1843, 2016. doi: 10.1021/acs.est.5b05337
- 34) S. Enami, Y. Sakamoto. OH-radical oxidation of surface-active *cis*-pinonic acid at the air–water interface. *J. Phys. Chem. A* 120: 3578–3587, 2016. doi: 10.1021/acs.jpca.6b01261
- 35) S. Enami, M. R. Hoffmann, A. J. Colussi. Extensive H-atom abstraction from benzoate by OH-radicals at the air–water interface. *Phys. Chem. Chem. Phys.* 18: 31505–31512, 2016. doi: 10.1039/C6CP06652F
- 36) S. Enami, M. R. Hoffmann, A. J. Colussi. OH-radical specific addition to glutathione S-atom at the air–water interface: Relevance to the redox balance of the lung epithelial lining fluid. *J. Phys. Chem. Lett.* 6: 3935–3943, 2015. doi: 10.1021/acs.jpcllett.5b01819
- 37) S. Enami, T. Fujii, Y. Sakamoto, T. Hama, Y. Kajii. Carboxylate ion availability at the air–water interface. *J. Phys. Chem. A* 120: 9224–9234, 2016. doi: 10.1021/acs.jpca.6b08868
- 38) S. Enami, A. J. Colussi. Long-range specific ion–ion interactions in hydrogen-bonded liquid films. *J. Chem. Phys.* 138: 184706, 2013.
- 39) S. Enami, A. J. Colussi. Long-range Hofmeister effects of anionic and cationic amphiphiles. *J. Phys. Chem. B* 117: 6276–6281, 2013. doi: 10.1021/jp401285f
- 40) S. Enami, M. R. Hoffmann, A. J. Colussi. Proton availability at the air/water interface. *J. Phys. Chem. Lett.* 1: 1599–1604, 2010. doi: 10.1021/jz100322w
- 41) H. Mishra, S. Enami, R. J. Nielsen, L. A. Stewart, M. R. Hoffmann, W. A. Goddard III, A. J. Colussi. Bronsted basicity of the air–water interface. *Proc. Natl. Acad. Sci. U.S.A.* 109: 18679–18683, 2012. doi: 10.1073/pnas.1209307109
- 42) P. A. J. Bagot, C. Waring, M. L. Costen, K. G. McKendrick. Dynamics of inelastic scattering of OH radicals from reactive and inert liquid surfaces. *J. Phys. Chem. C* 112: 10868–10877, 2008. doi: 10.1021/jp8024683
- 43) I. J. George, J. P. D. Abbatt. Heterogeneous oxidation of atmospheric aerosol particles by gas-phase radicals. *Nat. Chem.* 2: 713–722, 2010. doi: 10.1038/nchem.806
- 44) M. Roeselová, J. Vieceli, L. X. Dang, B. C. Garrett, D. J. Tobias. Hydroxyl radical at the air–water interface. *J. Am. Chem. Soc.* 126: 16308–16309, 2004. doi: 10.1021/ja045552m
- 45) J. Vieceli, M. Roeselova, N. Potter, L. X. Dang, B. C. Garrett, D. J. Tobias. Molecular dynamics simulations of atmospheric oxidants at the air–water interface: Solvation and accommodation of OH and O₃. *J. Phys. Chem. B* 109: 15876–15892, 2005.
- 46) M. Roeselová, P. Jungwirth, D. J. Tobias, R. B. Gerber. Impact, trapping, and accommodation of hydroxyl radical and ozone at aqueous salt aerosol surfaces. A molecular dynamics study. *J. Phys. Chem. B* 107: 12690–12699, 2003. doi: 10.1021/jp030592i
- 47) D. Manzanares, K. Rodriguez-Capote, S. Liu, T. Haines, Y. Ramos, L. Zhao, A. Doherty-Kirby, G. Lajoie, F. Possmayer. Modification of tryptophan and methionine residues is implicated in the oxidative inactivation of surfactant protein B. *Biochemistry* 46: 5604–5615, 2007. doi: 10.1021/bi062304p
- 48) V. K. Sharma, N. J. D. Graham. Oxidation of amino acids, peptides and proteins by ozone: A review. *Ozone Sci. Eng.* 32: 81–90, 2010. doi: 10.1080/01919510903510507
- 49) G. H. Xu, M. R. Chance. Hydroxyl radical-mediated modification of proteins as probes for structural proteomics. *Chem. Rev.* 107: 3514–3543, 2007. doi: 10.1021/cr0682047
- 50) C. A. Cassou, H. J. Sterling, A. C. Susa, E. R. Williams. Electrothermal supercharging in mass spectrometry and tandem mass spectrometry of native proteins. *Anal. Chem.* 85: 138–146, 2013. doi: 10.1021/ac302256d
- 51) C. A. Cassou, E. R. Williams. Anions in electrothermal supercharging of proteins with electrospray ionization follow a reverse Hofmeister series. *Anal. Chem.* 86: 1640–1647, 2014. doi: 10.1021/ac403398j
- 52) A. C. Susa, D. N. Mortensen, E. R. Williams. Effects of cations on protein and peptide charging in electrospray ionization from aqueous solutions. *J. Am. Soc. Mass Spectrom.* 25: 918–927, 2014. doi: 10.1007/s13361-014-0864-5
- 53) S. Milić, J. Bogdanović Pristov, D. Mutavdžić, A. Savić, M. Spasić, I. Spasojević. The relationship of physicochemical properties to the antioxidative activity of free amino acids in Fenton system. *Environ. Sci. Technol.* 49: 4245–4254, 2015. doi: 10.1021/es5053396
- 54) K. Y. C. Lee, J. Majewski, T. L. Kuhl, P. B. Howes, K. Kjaer, M. M. Lipp, A. J. Waring, J. A. Zasadzinski, G. S. Smith. Synchrotron X-ray study of lung surfactant-specific protein SP-B in lipid monolayers. *Biophys. J.* 81: 572–585, 2001.

- 55) S. Enami, M. R. Hoffmann, A. J. Colussi. Simultaneous detection of cysteine sulfenate, sulfinate, and sulfonate during cysteine interfacial ozonolysis. *J. Phys. Chem. B* 113: 9356–9358, 2009. doi: 10.1021/jp904316n
- 56) I. Spasojević, J. Bogdanović Pristov, L. Vujisić, M. Spasić. The reaction of methionine with hydroxyl radical: Reactive intermediates and methanethiol production. *Amino Acids* 42: 2439–2445, 2012. doi: 10.1007/s00726-011-1049-1
- 57) W. A. Pryor, R. M. Uppu. A kinetic-model for the competitive reactions of ozone with amino-acid-residues in proteins in reverse micelles. *J. Biol. Chem.* 268: 3120–3126, 1993.
- 58) M. R. M. Domingues, P. Domingues, A. Reis, C. Fonseca, F. M. Amado, A. J. Ferrer-Correia. Identification of oxidation products and free radicals of tryptophan by mass spectrometry. *J. Am. Soc. Mass Spectrom.* 14: 406–416, 2003. doi: 10.1016/S1044-0305(03)00127-2
- 59) Z. Maskos, J. D. Rush, W. H. Koppenol. The hydroxylation of tryptophan. *Arch. Biochem. Biophys.* 296: 514–520, 1992. doi: 10.1016/0003-9861(92)90605-V
- 60) A. P. Willard, D. Chandler. Instantaneous liquid interfaces. *J. Phys. Chem. B* 114: 1954–1958, 2010. doi: 10.1021/jp909219k
- 61) M. D. Baer, C. J. Mundy. Toward an understanding of the specific ion effect using density functional theory. *J. Phys. Chem. Lett.* 2: 1088–1093, 2011. doi: 10.1021/jz200333b
- 62) S. Enami, L. A. Stewart, M. R. Hoffmann, A. J. Colussi. Superacid chemistry on mildly acidic water. *J. Phys. Chem. Lett.* 1: 3488–3493, 2010. doi: 10.1021/jz101402y
- 63) B. Fiser, B. Jójárt, I. G. Csizmadia, B. Viskolcz. Glutathione-hydroxyl radical interaction: A theoretical study on radical recognition process. *PLoS One* 8: e73652, 2013. doi: 10.1371/journal.pone.0073652
- 64) B. Breiten, M. R. Lockett, W. Sherman, S. Fujita, M. Al-Sayah, H. Lange, C. M. Bowers, A. Heroux, G. Krilov, G. M. Whitesides. Water networks contribute to enthalpy/entropy compensation in protein–ligand binding. *J. Am. Chem. Soc.* 135: 15579–15584, 2013. doi: 10.1021/ja4075776
- 65) V. Gupta, K. S. Carroll. Sulfenic acid chemistry, detection and cellular lifetime. *Biochim. Biophys. Acta* 1840: 847–875, 2014. doi: 10.1016/j.bbagen.2013.05.040
- 66) K. G. Reddie, K. S. Carroll. Expanding the functional diversity of proteins through cysteine oxidation. *Curr. Opin. Chem. Biol.* 12: 746–754, 2008. doi: 10.1016/j.cbpa.2008.07.028
- 67) L. Turell, H. Botti, S. Carballal, G. Ferrer-Sueta, J. M. Souza, R. Durán, B. A. Freeman, R. Radi, B. Alvarez. Reactivity of sulfenic acid in human serum albumin. *Biochemistry* 47: 358–367, 2008. doi: 10.1021/bi701520y
- 68) T. Nakamura, T. Yamamoto, M. Abe, H. Matsumura, Y. Hagihara, T. Goto, T. Yamaguchi, T. Inoue. Oxidation of archael peroxiredoxin involves a hypervalent sulfur intermediate. *Proc. Natl. Acad. Sci. U.S.A.* 105: 6238–6242, 2008. doi: 10.1073/pnas.0709822105
- 69) M. Sarker, J. Rose, M. McDonald, M. R. Morrow, V. Booth. Modifications to surfactant protein B structure and lipid interactions under respiratory distress conditions: Consequences of tryptophan oxidation. *Biochemistry* 50: 25–36, 2011. doi: 10.1021/bi101426s